Silk Fiber Formation after High-Pressure Treatment of Fibroin Solution in a Diamond Anvil Cell

Ronald Gebhardt, Charlotte Vendrely,† Michael Hanfland, and Christian Riekel*

European Synchrotron Radiation Facility, B.P. 220, F-38043 Grenoble Cedex, France

Received August 18, 2008
Revised Manuscript Received November 1, 2008

During silk spinning by silk worms and spiders, aqueous fibroin protein solution is converted into silk II type filaments.[1,2] The conversion process is driven by changes in pH, cations concentration, dope concentration, and shearing effects in the spinning duct.[1,2] Structural models of silk II fibers based on X-ray and neutron scattering techniques suggest a hierarchical organization of antiparallel β-sheet and short-range order domains forming nanofibrils in a random protein matrix.[3−8]

β-Sheet formation in silk fiber assembly shows structural similarities to cross-β sheet formation in amyloid fibril assembly. At the origin is a partially unfolded protein, which like fibroin either exists in its native form[9] or has been formed by misfolding.[10] A prefibrillar state with increased structural order seems to be essential in both cases. The formation of a fibroin aggregate preceding ordered β-sheet material formation has been suggested by several in vitro studies.[11−14] Modeling of amyloid formation in aqueous environment suggests a two-step condensation-ordering mechanism of peptide chains into an intermediary oligomeric aggregate followed by the formation of an ordered cross-β structure.[15] The direct formation of cross-β assemblies is a special case, realized at low peptide concentration[15,16] (for further experimental data see ref 15).

In most of the cases the action of high pressure on protein oligomers induces association/dissociation reactions including amyloid fibril formation.[17,18] Since generally the monomers occupy a smaller volume, protein complexes tend to dissociate under high pressure. As with conformational changes, the global volume change of a dissociation reaction is the sum of several contributions such as intra- and intermolecular interactions and solvation contributions.[19,20] Hydrostatic pressure weakens electrostatic interactions between protein subunits due to electrostriction. On the other hand, the strength of hydrophilic bonds are increased due to the shortening of bonding length.[21] Preferred protein−water interactions lead to hydration of proteins. As a consequence, unfolded or partly folded protein conformations with a higher accessible surface area for water are stabilized under pressure.[22] High-pressure experiments offer therefore the unique possibility to increase the population of partially folded amyloidogenic intermediates[22] without a preceding aggregation step, resulting in disordered aggregates.[23] After pressure release the subsequent formation of amyloid fibrils or amorphous aggregates has been studied (see for example refs 24 and 25). Different types of quaternary fibrillar folds have been observed, ranging from straight strands to wound, branched and circularly shaped amyloidic fibrils.[18,26] The pressure stability of fibers ranges from highly susceptible to insensitive depending on their hydration states and molecular packing.[27,28] In view of the analogies between silk II fiber and amyloid fibril assembly, we were interested verifying whether fibroin solution would behave in a similar way upon pressure treatment.

Fibroin solution was prepared from *Bombyx mori* cocoons as described elsewhere[14] (see also Supporting Information). The solution was pressurized up to 700 MPa at 293 K in a diamond anvil cell (DAC).[29] After decompression the cell was opened, and the formed aggregate or fibrous material formation was studied by Raman spectroscopy. For this the fibrous material was dried on the diamond window of the DAC. Details on the DAC cell performance, the Raman spectrometer, and the analysis of the Raman spectra are reported in the Supporting Information.

Figure 1A−D shows micrographs of the pressure-generated fibers at ambient pressure after a pressure treatment at 700 MPa for 5 h. Single straight fibers of 300 μm length and 3 μm diameter are observed. Some fibers show branching with Y- and T- shaped junctions (Figure 1B,C). A similar branching has also been observed for amyloid fibril formation.[18] Besides single and branched fibers more disordered networks of fibers can also be observed (Figure 1D). Figure 2 shows the Raman spectra obtained from the fibers after incubation of fibroin solution at 100 or 700 MPa. A zoom in the region sensitive to the silk I/II transformation (1070−1090 cm^{-1}) is shown in Figure 3A. The bands at 1103 and 1083 cm^{-1} are attributed to a silk I α-helical intermediate[30] and silk II β-sheets.[31] Our data suggest that after a pressure treatment of 100 MPa silk I is generated. By contrast, silk II has been formed after a pressure treatment of 700 MPa. An evolution to a more hydrophilic environment of the tyrosine groups is suggested by the band in the range 830−850 cm^{-1}.[32] During this process, tyrosine groups buried in an α-helical environment could rearrange into a more accessible β-sheet environment. The analysis of the amide I band (Figure 3B) is complicated by the multiple contributions to this band.[33] The amide I band was decomposed using 11 and 12

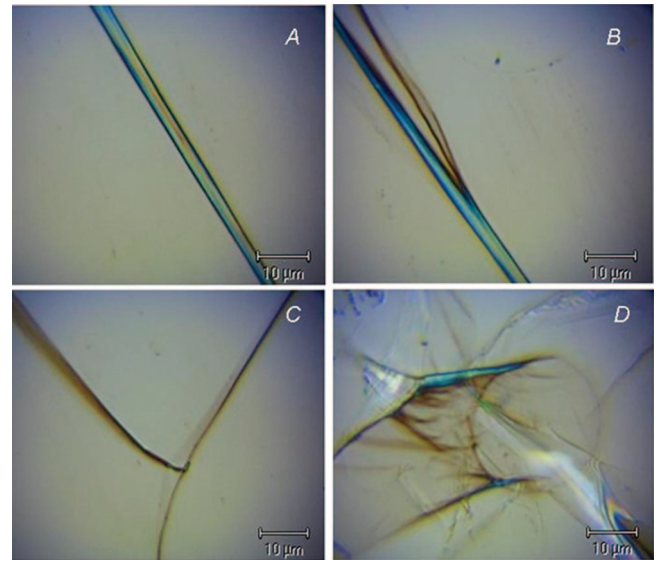

Figure 1. Micrographs of fibrous material found in a diamond anvil cell after pressure treatment of a fibroin solution: (A) single fiber with a diameter of 3 μm; fiber with a Y-shaped junction (B) and a T-shaped junction (C); disordered network of fibers (D).

* To whom correspondence should be addressed.
† Present address: Université de Cergy-Pontoise, ERRMECE, F-95000, Cergy-Pontoise, France.

10.1021/ma801872m CCC: $40.75
Published on Web 11/24/2008

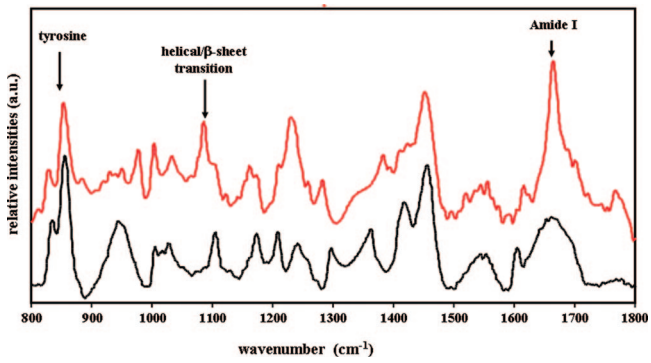

Figure 2. Raman spectra of fibers obtained from fibroin solutions incubated at 100 MPa (black) and 700 MPA (red).

components for the silk I and silk II type spectra, respectively. Bands at 1664 and 1669 cm^{-1} are assigned to β-sheet conformation.[30,31] The bands at 1643/1644 cm^{-1} and those at 1680−1709 cm^{-1} correspond to peptide bonds in type I and type III β-turns.[34] Assignment of the other bands is less straightforward. While the band at 1659 cm^{-1} could correspond to an unordered structure,[30] further assignments were done for the bands at 1651 cm^{-1} (α-helices[35]) and 1634/1636 cm^{-1} (β-turns, β-sheet or unordered structures[34]) as well as for the bands between 1600 and 1624 cm^{-1} (vibrations of the aromatic amino acids, including tyrosine side chains[34]). The Raman spectra shown in Figure 3B were decomposed into almost the same bands. The upper spectrum shows a supplementary band at 1664 cm^{-1}, corresponding to β-sheet conformation. The β-sheet content was analyzed in detail. The fractions of secondary structure were determined using the relative areas of the single bands. The analysis revealed 30% β-sheet structures in the upper spectrum of Figure 3B and 17% β-sheet structure for the spectrum shown below. In contrast, the estimated percentages for unordered structures were 17% and 30%, respectively. About equal results were obtained in case of the β-turns (43% and 48%, respectively) and the α-helix content (10% and 6%, respectively). According to the analysis of the Raman spectra, the fibrous material formed after a high-pressure treatment of 700 MPa correspond to silk II structure. In contrast, the aggregates formed after a treatment of 100 MPa show similarities to a silk I spectrum.

On the basis of research into high-pressure effects on amyloid fibril formation[22] and similarities to silk fiber formation mentioned above, we can speculate about a possible reaction mechanism under pressure. First, the secondary structure of fibroin should unfold under high pressure due to penetration of water molecules and protein hydration.[22] The resulting fibroin conformation differs from the original fibroin conformation in its high aggregation propensity. After pressure release protofibrils could be formed[10] which assemble to silk II fibers at ambient pressure.

In conclusion, we have shown the formation of silk II fibers at ambient pressure after a high-pressure treatment of 700 MPa. The minimum-pressure treatment which is necessary to generate silk II fibers has not yet been determined. It is, however, evident that a high-pressure treatment of 100 MPa is not sufficient to generate silk II, since only amorphous aggregates (picture not shown) with a silk I type Raman spectrum were observed. The observation of silk II fiber formation after high pressure implies a higher volume of the silk II fiber compared to the state of fibroin under high pressure, which could be attributed to water excluded cavities in the fiber in analogy to amyloid fibril formation.[23]

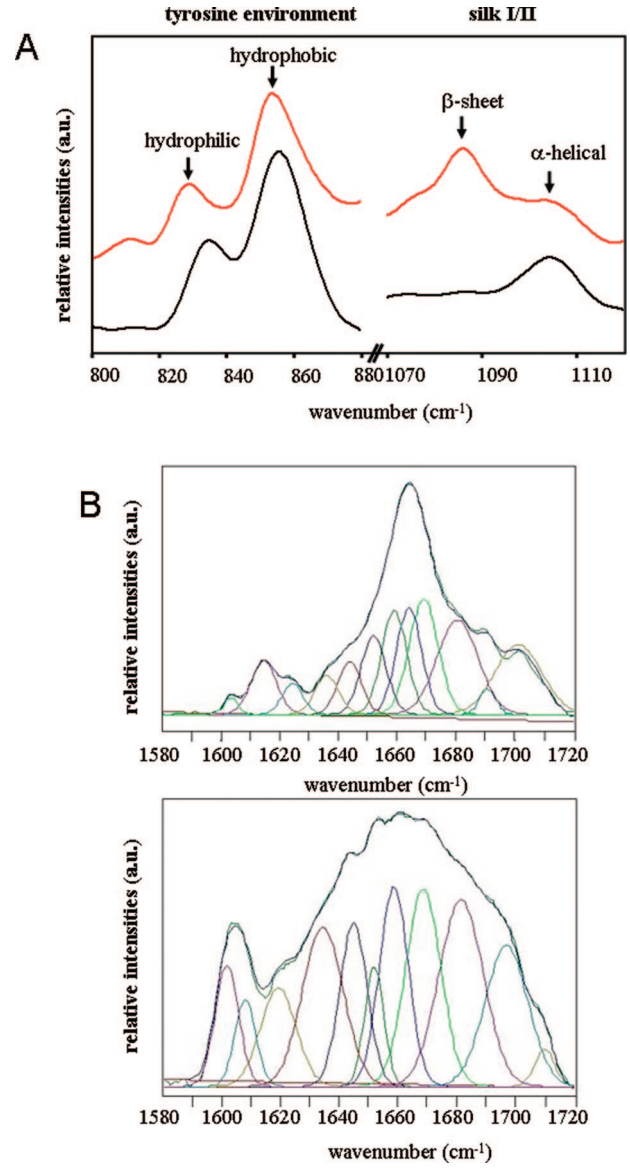

Figure 3. (A) Zoom into the range 800−1110 cm^{-1} range; the black curve corresponds to silk I type material obtained after 100 MPa pressure treatment; the red curve corresponds to silk II type material obtained after 700 MPa pressure treatment. (B) Spectral deconvolution of amide I band for silk I type material (lower picture) and silk II type material (upper picture) (see text and Supporting Information). The experimental data curve (in green) and the global fitted curve (in blue) are largely overlapping. The colors of the individual fitted curves have been chosen for a better visual separation.

Acknowledgment. We thank R. Davies and A. Martel (ESRF) for help with the use of the Raman setup and the interpretation of the spectra. J. Jacobs and M. Mezouar (ESRF) provided constant support with the use of the DAC. The authors acknowledge financial support from the FP6 SAXIER grant.

Supporting Information Available: Fibroin preparation, DAC cell pressure precision, Raman spectrometer, and Raman spectra analysis. This material is available free of charge via the Internet at http://pubs.acs.org.

References and Notes

(1) Vollrath, F.; Knight, D. P. *Nature (London)* **2001**, *410*, 541–548.
(2) Magoshi, J.; Magoshi, Y.; Nakamura, S. In *Silk Polymers. Materials Science and Biotechnology*; Kaplan, D., Adams, W. W., Farmer, B., Viney, C., Eds.; ACS Symposium Series 544; American Chemical Society: Washington, DC, 1994; pp 292−310.

(3) Martel, A.; Burghammer, M.; Davies, R. J.; Riekel, C. *Biomacromolecules* **2007**, *8*, 3548–3556.
(4) Grubb, D. T.; Jelinski, L. W. *Macromolecules* **1997**, *30*, 2860–2867.
(5) Yang, Z.; Grubb, D. T.; Jelinski, L. W. *Macromolecules* **1997**, *30*, 8254–8261.
(6) Sapede, D.; Seydel, T.; Forsyth, T.; Koza, M. M.; Schweins, R.; Vollrath, F.; Riekel, C. *Macromolecules* **2005**, *38*, 8447–8453.
(7) Miller, L. D.; Putthanarat, S.; Eby, R. K.; Adams, W. W. *Int. J. Mol. Biol.* **1999**, *24*, 159–165.
(8) Putthanarat, S.; Stribeck, N.; Fossey, S. A.; Eby, R. K.; Adams, W. W. *Polymer* **2000**, *41*, 7735–7747.
(9) Kaplan, D. L.; Lombardi, S. J.; Muller, W. S.; Fossey, S. A.; Silks: chemistry, properties and genetics. In *Biomaterials, novel materials from biological sources*; Byrom, D. Ed.; Stockton Press: New York, 1991; pp 3−53.
(10) Dobson, C. M. *Nature (London)* **2003**, *426*, 884–890.
(11) Jin, H. J.; Kaplan, D. L. *Nature (London)* **2003**, *424*, 1057–1061.
(12) Rammensee, S.; Slotta, U.; Scheibel, T.; Bausch, A. R. *Proc. Natl. Acad. Sci. U.S.A.* **2008**, *105*, 6590–6595.
(13) Roessle, M.; Panine, P.; Urban, V. S.; Riekel, C. *Biopolymers* **2004**, *74*, 316–327.
(14) Martel, A.; Burghammer, M.; Davies, R.; DiCola, E.; Panine, P.; Salmon, J. B.; Riekel, C. *Biomicrofluidics* **2008**, *2*, 024104−024107.
(15) Auer, S.; Dobson, C. M.; Vendruscolo, M. *HFSP J.* **2007**, *1*, 137–146.
(16) Nelson, R.; Sawaya, M. R.; Balbirnie, M.; Madsen, A. Ø.; Riekel, C.; Grothe, R.; Eisenberg, D. *Nature (London)* **2005**, *435*, 773–778.
(17) Torrent, J.; Alvarez-Martinez, M. T.; Harricane, F.; Heitz, F.; Liautard, J. P.; Balny, C.; Lange, R. *Biochemistry* **2004**, *43*, 7162–7170.
(18) Jansen, R.; Grudzielanek, S.; Dzwolak, W.; Winter, R. *J. Mol. Biol.* **2004**, 203–206.
(19) Royer, C. A.; Balny, C.; Masson, P.; Heremans, K. *Biochim. Biophys. Acta* **2002**, *1595*, 201–209.
(20) Balny, C. *Biochim. Biophys. Acta* **2006**, *1764*, 632–639.
(21) Silva, J.; Weber, G. *Annu. Rev. Phys. Chem.* **1993**, *44*, 89–113.
(22) Meersman, F.; Dobson, C. M.; Heremans, K. *Chem. Soc. Rev.* **2006**, *35*, 908–917.
(23) Foguel, D.; Silva, J. L. *Biochemistry* **2004**, *43*, 11361–11370.
(24) Gorovits, B. M.; Horowitz, P. M. *Biochemistry* **1998**, *37*, 6132–6135.
(25) Meersman, F.; Smeller, L.; Heremanns, K. *Biophys. J.,* **2002**, *82*, 2635–2644.
(26) Harper, J. D.; Lieber, C. M.; Lansbury, P. T. *Chem. Biol.* **1997**, *4*, 951–959.
(27) Dirix, C.; Meersman, F.; MacPhee, C. E.; Dobson, C. M.; Heremans, K. *J. Mol. Biol.* **2005**, *347*, 903–909.
(28) Cordeiro, Y.; Kraineva, J.; Ravindra, R.; Lima, L. M. T. R.; Gomes, M. P. B.; Foguel, D.; Winter, R.; Silva, J. L. *J. Biol. Chem.* **2003**, *279*, 5346–5352.
(29) Gebhardt, R.; Hanfland, M.; Mezouar, M.; Riekel, C. *Biomacromolecules* **2007**, *8*, 2092–2097.
(30) Monti, P.; Taddei, P.; Freddi, G.; Asakura, T.; Tsukada, M. *J. Raman Spectrosc.* **2001**, *32*, 103–107.
(31) Rousseau, M. E.; Lefèvre, T.; Beaulieu, L.; Asakura, T.; Pézolet, M. *Biomacromolecules* **2004**, *5*, 2247–2257.
(32) Siamwiza, M. N.; Lord, R. C.; Chen, M. C.; Takamatsu, T.; Harada, I.; Shimanouchi, H. M. *Biochemistry* **1975**, *14*, 4870–4876.
(33) Lefevre, T.; Rousseau, M. E.; Pezolet, M. *Biophys. J.* **2007**, *92*, 2885–2895.
(34) Rousseau, M. E.; Beaulieu, L.; Lefevre, T.; Paradis, J.; Asakura, T.; Pezolet, M. *Biomacromolecules* **2006**, 7.
(35) Wen, A. *J. Pharm. Sci.* **2007**, *96*, 2861–2878.

MA801872M